Journal of Thermal Analysis and Calorimetry (2024) 149:7215–7224
https://doi.org/10.1007/s10973-024-13266-6

Semi-dry carbonated recycled concrete paste as alternative to limestone and its reactivity in LC^3

Yu Jin[1] · Zihan Xiong[2] · Weipeng Feng[1] · Dapeng Zheng[2,3] · Serina Ng[4] · Yaocheng Wang[2,3,5]

Received: 17 October 2023 / Accepted: 30 April 2024 / Published online: 3 June 2024

Abstract

Recycled concrete paste (RCP) can be transformed to the carbonated RCP (cRCP) as supplementary cementitious materials (SCM). By blending cRCP with calcined clay prepared from excavated waste, a distinctive limestone calcined clay cement (LC^3) was produced. The aim of this research was to assess the reactivity of LC^3 produced from the cRCP utilizing different carbonation procedures, via isothermal calorimetry. The carbonation process occurred at 100% R.H. and 20 vol.% CO_2 concentration. To investigate the effect of pre-wetting treatment on the carbonation degree, the RCP was pre-wetted using either deionized water or 0.1 mol L^{-1} NaOH solution. The carbonation degree and microstructure of cRCP were analyzed using thermogravimetric analysis, X-ray diffraction, and solid-state nuclear magnetic resonance. The results revealed that pre-wetting methods significantly impact carbonation degree, while the alkali solutions had moderate influence. Notably, the pre-wetting procedure aided in decalcifying other hydrates apart from portlandite, leading to compositional variations within the cRCP. Nevertheless, these variations did not significantly affect the cRCP's reactivity in LC^3.

Keywords Carbon capture utilization · Recycled concrete fines · Low-carbon cement · Heat of hydration

Introduction

The cement industry in China emitted approximately 1.3 billion tons of CO_2 in 2020 [1], about 13% anthropogenic CO_2 emission in China annually, representing a significant obstacle in accomplishing the country's goal of achieving 'carbon peak and carbon neutrality'. The United Nations Environment Programme (UNEP) highlighted the production of composite cements, which contain high blends of supplementary cementitious materials (SCM), as a strategy for reducing CO_2 emissions in the cement industry in the next 30 years [2].

Recycled concrete paste (RCP) refers to the fine fraction that results from the recycling of demolished concrete, obtained during the production of recycled aggregates. RCP mainly comprises hydrated cement paste and the fine fraction of aggregates [3]. CO_2 mineralization of RCP into SCM has been introduced as a new technique for carbon capture and utilization (CCU) [4], which is one of the most common treatments to improve RCP's reactivity [5]. The hydration products such as portlandite, calcium silicate hydrate gel, and ettringite react with CO_2 to form various types of $CaCO_3$ (calcite, vaterite, aragonite, or amorphous $CaCO_3$) and alumina–silica gel [5]. The cement composite that results from the carbonated RCP (cRCP) demonstrates higher strength compared to that of limestone, due to the formation of calcium carboaluminate hydrate, suggesting its viability as SCM [5, 6].

Various carbonation methods have been suggested, either on realistic recycled concrete fines [7] or on simulated recycled concrete paste, to comprehensive understand the carbonation mechanism. The RCP was carbonated under mild

✉ Yaocheng Wang
wangyc@szu.edu.cn

1 Institute of Technology for Marine Civil Engineering, Shenzhen Institute of Information Technology, Shenzhen 518172, China

2 Present Address: College of Civil and Transportation Engineering, Shenzhen University, Shenzhen 518060, China

3 Key Laboratory for Resilient Infrastructures of Coastal Cities (MOE), College of Civil and Transportation Engineering, Shenzhen University, Shenzhen 518060, China

4 Shijiazhuang ChangAn Yucai Building Materials Co. Ltd, Shijiazhuang 051431, China

5 Guangdong Provincial Key Laboratory of Durability for Marine Civil Engineering, Shenzhen University, Shenzhen 518060, China

conditions of 65% R.H., 20°C, and 20% CO_2 concentration [8]. This is regarded as a typical accelerated carbonation setup for investigating the carbonation resistance of concrete. After 28 days of carbonation, approximately 17% $Ca(OH)_2$ remained in the RCP, indicating a relatively low carbonation efficiency. Wet carbonation in an alkaline solution resulted in a 90% carbonation degree within 2 h. Additionally, the carbonation products were impervious to the initial phase composition of the RCP, suggesting that scaling up the wet method to an industrial level is feasible [9]. Alkali in the solution facilitated CO_2 dissolution, initially expediting carbonation, but then hampering it due to its adverse impact on hydrate dissolution. Increased alkali concentration had no bearing on the overall carbonation efficiency for the wet method [10]. Increased alkali concentrations resulted in larger calcite crystals, whereas alkali concentration had only a minor impact on the composition or structure of the alumina–silica gel [11]. While the wet method is an efficient carbonation method, it requires energy for agitation and more procedures for liquid–solid separation and drying. As a result, a semi-dry method was developed by exposing the RCP to a humid atmosphere. Research discovered that the relative humidity was pivotal to carbonation efficiency, where the carbonation degree increased from 31% at 80% R.H. to 66% at 100% R.H. in a span of 5 h. The influence of CO_2 concentration was lighten, as shown in reference [12]. The transport of CO_2 in water is sluggish, yet liquid water is advantageous for transporting of the other reactants. The semi-dry method, while disadvantaged by the densification effect of carbonation products, still attained a carbonation efficiency lower than the wet method. However, it represented a trade-off between carbonation efficiency and ease of processing.

Ternary composite cements comprising Portland cement, metakaolin, cRCP, or RCP have recently been investigated [13, 14]. In the composite cement with 10% metakaolin and 30% cRCP, alumina–silica gel facilitated portlandite consumption and calcium carbonate stabilized ettringite content, resulting in high reaction degree and compressive strength at early ages [13]. It was demonstrated that the alumina–silica gel formed by carbonation does not hinder the hydration of metakaolin or vice versa. In the composite cement with 30% metakaolin and RCP, a synergistic effect with respect to reaction kinetics and mechanical strength was observed, when the mass ratio between metakaolin and RCP was 2:1, regardless of the mineralogical composition of the RCPs [14]. These findings highlight the importance of the concurrent use of reactive alumina–silica and calcium carbonate sources.

Limestone calcined clay cement (LC^3) comprises calcined clay and limestone powder, which contains both reactive alumina–silica and calcium carbonate as SCM [15]. As a low-carbon cement, it is readily available, simple to produce, and capable of reducing CO_2 emissions by up to 50% compared to Portland cement [16]. Over 1 billion tons of construction and demolition waste (CDW) are produced annually in China [17], mainly in the form of excavated waste soil (approx. 70%) and inert CDW (approx. 30%) such as concrete debris. Therefore, the substitution of cRCP and excavated soil for limestone and clay in the manufacturing of LC^3 is advantageous.

This study aims to understand the collective influence of semi-dry and alkaline conditions on RCP carbonation degree. Additionally, the potential for cRCP as an alternative to limestone in LC^3 will be assessed. Research indicates that calcined clay and limestone yield a synergistic effect on the performance of LC^3 [18]. Nonetheless, it is uncertain whether employing cRCP instead of limestone would adversely affect the performance of LC^3. The heat of hydration is a sensitive indicator of the reactivity of cementitious materials [19]. A significant correlation existed between the heat of hydration after 3 days and the compressive strength of cementitious materials after 28 days [20]. Thus, the heat of hydration will be used to evaluate the reactivity of cRCP in LC^3 in this study.

Materials and methods

Materials

The cement used in this study was a P I 52.5 Portland cement (comparable to CEM I 52.5N). Raw clay was made from an excavated soil in Shenzhen. Raw clay sources like excavated clay can be used as raw materials to produce LC^3 [21] or composite cement [22]. In this study, excavated soil was used as clay source by means of wet separation. The excavated soil was initially mixed with tap water to create a suspension. The suspension underwent filtration through a sieve with a pore diameter of 75 µm. Further separation was achieved by sedimentation of the filtered suspension. The sediment was dried in an oven operating at 105 °C. Following the drying process, the sieved soil was ground and subjected to analysis via X-ray diffraction (XRD) and thermogravimetric analysis (TGA). Following the analysis, the sieved soil was composed of kaolinite, illite, and quartz. The kaolinite content was determined to be 67.8% via TGA using the tangential method [23]. To obtain the calcined clay, the sieved soil was calcined within a muffle furnace at 800°C for a duration of 2 h. The workflow for the preparation of the calcined clay presents in Fig. 1a. Based on the BET method, the surface area of the calcined clay was found to be 15.8 $m^2\ g^{-1}$.

The chemical compositions of the cement and the calcined clay were determined by means of Thermo Fisher

Fig. 1 Workflow for the preparation of **a** the calcined clay and **b** the cRCP

Table 1 The chemical composition of the cement and calcined clay/%

	CaO	SiO_2	Al_2O_3	Fe_2O_3	MgO	SO_3	K_2O	Na_2O	TiO_2	LOI
Cement	67.0	18.6	5.4	3.0	1.3	3.1	0.5	0.3	0.4	2.2
Calcined clay	0.2	49.5	43.6	4.4	0.5	N.A	1.1	N.A	N.A	1.2

ARL PERFORM'X sequential XRF and quantitatively analyzed using UniQuant software (Table 1).

Carbonation of the RCP

The RCP was simulated using hydrated and ground cement paste. The hydrated cement paste was produced with a water-to-cement ratio of 0.35 and was cured in a climatic chamber at over 90% R.H. and 20 ± 2 °C for 28 days, similar with the procedure described in the literature but with a shorter curing period [24]. The hydrated cement paste was then crushed and mechanically ground to pass through a 75-μm pore diameter sieve to serve as the starting material for the carbonation experiment. The BET surface area of the RCP was 6.3 $m^2\ g^{-1}$.

Carbonating the RCP involved varying parameters, as stated in Table 2. The RCP was positioned horizontally in a tray with an approximate depth of 1 mm. To pre-wet the samples in the semi-dry method, different solid–liquid ratios of deionized water were sprayed on top. In the semi-dry with lye method, 0.1 mol L^{-1} NaOH solution was utilized. The sample tray was then put into a carbonation chamber for 30–180 min, where the CO_2 concentration was 20%, and the relative humidity and temperature were 100% and 20 ± 2 °C, respectively. It is important to acknowledge that the utilization of 100% R.H. in this study renders the dry method as nominal. The workflow for the preparation of the cRCP presents in Fig. 1b.

Table 2 Full-factorial design of carbonation experiment

Method	Liquid–solid ratio for pre-wetting	Lye concentration / mol L^{-1}	Time/min	Number of the cRCP
Dry	0	0	30, 60, 120, 180	4
Semi-dry	0.01, 0.05, 0.1	0	30, 60, 120, 180	12
Semi-dry with lye	0.01, 0.05, 0.1	0.1	30, 60, 120, 180	12

The theoretical carbonation degree was suggested to be calculated based on the mass fractions of all alkaline (earth) oxides in cement except CaO in gypsum [25]:

$$\omega_{\text{theoretical,CO}_2} = \frac{M_{\text{CO}_2}}{M_{\text{CaO}}} \times \left(\omega_{\text{CaO}} - 0.7 \times \omega_{\text{SO}_3}\right) + 0.71 \times \omega_{\text{Na}_2\text{O}} + 0.4675 \times \omega_{\text{K}_2\text{O}} \quad (1)$$

where ω is the mass fraction of the oxides listed in Table 1, and M is the molar mass of the oxides.

The carbonation degree can be calculated based on the measured CO_2 content in the cRCP and the theoretical carbonation degree:

$$\eta_{\text{carbonation degree}} = \frac{(1 + w/c) \times \omega_{\text{measured, CO}_2}}{\left(1 - \omega_{\text{measured, CO}_2}\right) \times \omega_{\text{theoretical, CO}_2}} \quad (2)$$

where w/c is the water-to-cement ratio used in the preparation of the RCP.

Methods

Characterization of the cRCP

The content of $CaCO_3$ and $Ca(OH)_2$ content in the cRCP was determined using TGA by employing the tangential

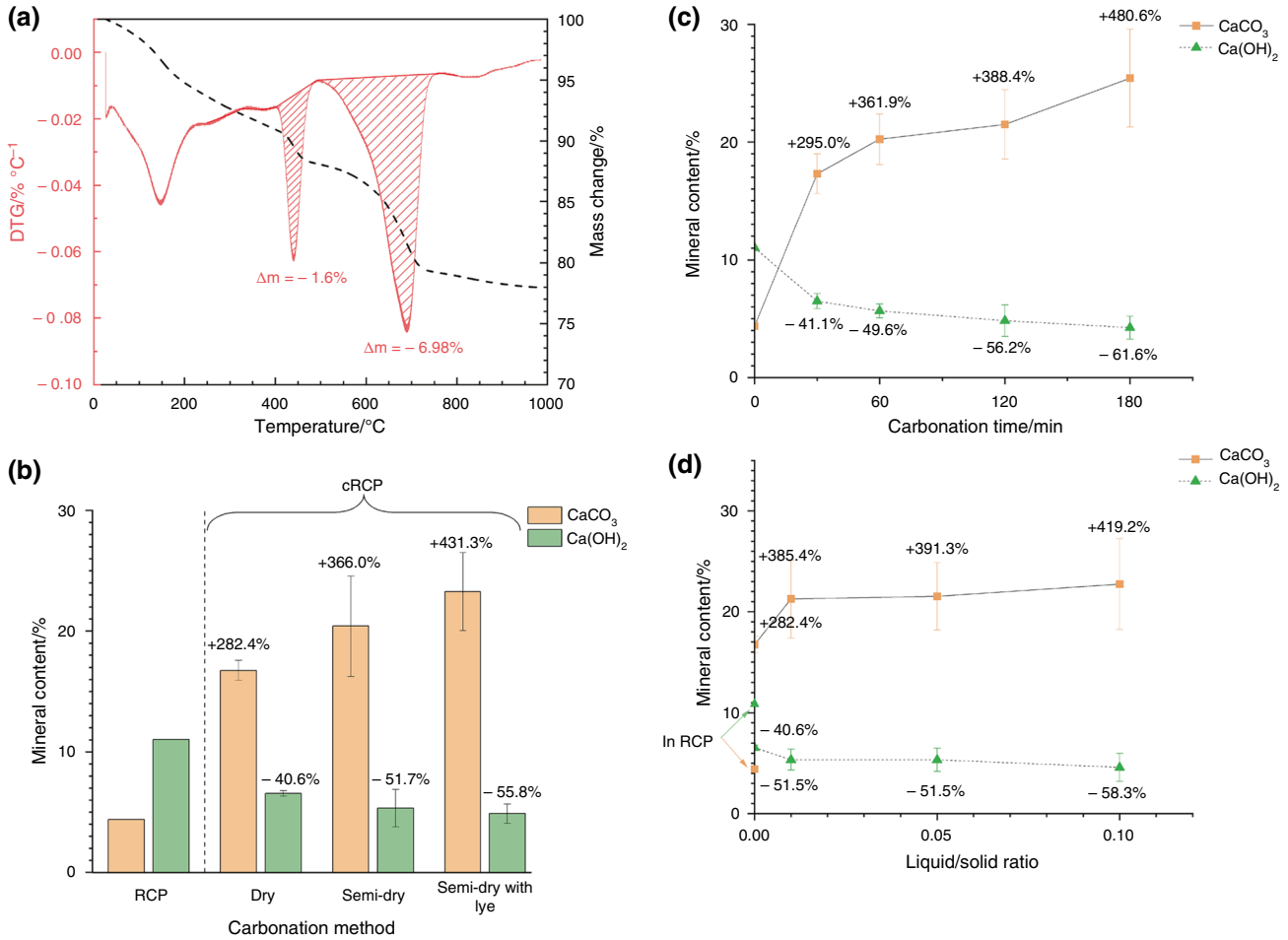

Fig. 2 **a** Determination of the $CaCO_3$ and $Ca(OH)_2$ content in the cRCP by TGA using the tangential method; the effect of: **b** carbonation method; **c** carbonation time; and **d** liquid–solid ratio on the mineral content in the cRCP (The numbers above the data points are the difference between the carbonated and uncarbonated RCP)

method, which is illustrated in Fig. 2a. Measurements were conducted using a Netzsch STA 449 F3 under a N_2 atmosphere and with a gas flow rate of 30 mL min^{-1} and a heating rate of 10 K min^{-1}.

For XRD analysis, a Bruker D8 Advance X-ray diffractometer was used, operating at 40 kV and 40 mA, employing Cu-Kα radiation ($\lambda = 1.5406$ Å) in the θ–2θ configuration with an angular scan range from 5 to 70° 2θ. The scan step was 0.0190° and lasted for 19.2 s.

The spectra for ^{29}Si- and ^{27}Al NMR spectra were obtained using at the JEOL JNM-ECZ 600R NMR spectrometer with a magnetic field strength of 14.1 T. The measurements for ^{29}Si- and ^{27}Al-NMR were taken in 8-mm zircon rotors at a spin rate of 6 kHz and 3.2-mm zircon rotors at a spin rate of 15 kHz, respectively. 90° pulses were used in single-pulse mode with a repetition time of 60 s for ^{29}Si-NMR and 5 s for ^{27}Al-NMR measurements. Trimethylsilylpropanoic acid (TSP) and $AlK(SO_4)_2 \cdot 12H_2O$ were used as standard reference for the chemical shift at 1.459 ppm in the ^{29}Si spectra and at -0.21 ppm in the ^{27}Al spectra, respectively. The instrument software JEOL Delta was used to process the acquired 1D spectra.

Reactivity of the cRCP in LC^3

In this study, the LC^3 mixed with 53% cement, 30% calcined clay, 15% limestone, and additional 2% gypsum. The limestone was substituted with the cRCP to prepare the unique LC^3 produced from CDW. The BET surface area of the limestone was 3.9 $m^2\ g^{-1}$. The BET surface area of the cRCP treated through the dry method was 6.3 $m^2\ g^{-1}$, while the surface area of the cRCP treated with semi-dry methods spanned between 8 and 8.1 $m^2\ g^{-1}$.

The samples' reactivity was assessed through the quantification of the heat of hydration, using isothermal calorimetry. The samples were prepared with a water-to-solid ratio of 0.4, while 0.2% PCE superplasticizer was added. At 20°C, the heat flow was monitored using TA Instruments TAM Air. To prepare the test samples, 3 g of powder was mixed with 1.2-mL water in a 10-mL vial and vortex stirred for 1 min. The measurement lasted for 72 h.

Results and discussion

Carbonation of the RCP

Prior to the carbonation experiment, the RCP underwent natural carbonation via atmospheric CO_2, resulting in $CaCO_3$ and $Ca(OH)_2$ contents of 4.4 g per 100-g RCP and 11.0 g per 100-g RCP, respectively. Following the carbonation experiment, the $CaCO_3$ content of cRCP processed using the dry method was considerably lower than that of the semi-dry methods, while the semi-dry with lye method demonstrated higher carbonation efficiency than the semi-dry method (refer to Fig. 2b). Equation (2) reveals that the cRCP achieved a maximum carbonation degree of 41%, corresponding to 30.8-g $CaCO_3$ per 100-g cRCP. Samples processed using the three carbonation methods achieved average carbonation degrees of 21%, 26%, and 30%, respectively. It was reported in the literature [12] that the maximum carbonation degree of the semi-dry method was 61% at 100% R.H., which utilized vibrating sieves during the carbonation process. Nonetheless, the semi-dry and alkaline conditions did enhance the carbonation degree in the RCP. The disproportionate increase in $CaCO_3$ content and decrease in $Ca(OH)_2$ content in the cRCP indicated that carbonation of $Ca(OH)_2$ (portlandite) was not the primary source of $CaCO_3$ incrementation. Therefore, the pre-wetting treatment was advantageous for the carbonation of hydration products such as calcium silicate hydrate (C-S-H) gel and ettringite, rather than portlandite.

As the carbonation time increases, the $CaCO_3$ content in the cRCP increases while the $Ca(OH)_2$ content decreases gradually (Fig. 2c). The lengthening of the carbonation time appears to have a negligible impact on the carbonation of $Ca(OH)_2$, but has a significant effect on other hydration products. The dissolution of $Ca(OH)_2$ in the pore solution protects C-S-H gel from carbonation [26]. The only explanation for this phenomena is that CO_2 diffusion was impeded by the carbonation products deposited on the outer shell, as carbonation of hardened cement paste caused a compact microstructure in the hardened paste [27].

The liquid–solid ratio is a key factor in determining the carbonation degree. Although the experimental conditions in this study maintained a high humidity, the formation of $CaCO_3$ is to some extent influenced by the pre-wetting treatment. As the liquid–solid ratio increased to 0.01, the $CaCO_3$ content increased significantly, while the higher ratio did not largely contribute to the increase in the $CaCO_3$ content. A big margin of error on the $CaCO_3$ content was observed, indicating the importance of carbonation time and alkali environment for the carbonation of the hydration products besides portlandite (see Fig. 2d).

Microstructural evolution in the cRCP

In the field of silicate chemistry, Q^n species are utilized to indicate the polymerization degree of SiO_4, with the value of n indicating the number of bridging oxygen present in a single SiO_4 tetrahedron. The ^{29}Si NMR spectrum shows peaks found at −71 ppm, −79 ppm, and −84 ppm (Fig. 3a), which are recognized as Q^0, Q^1, and Q^2 species, respectively [28]. Q^0 originates from belite (dicalcium silicate or C_2S) in the anhydrous cement while Q^1 and Q^2 are located at the pair or corner sites in C-S-H gel. Carbonation facilitated

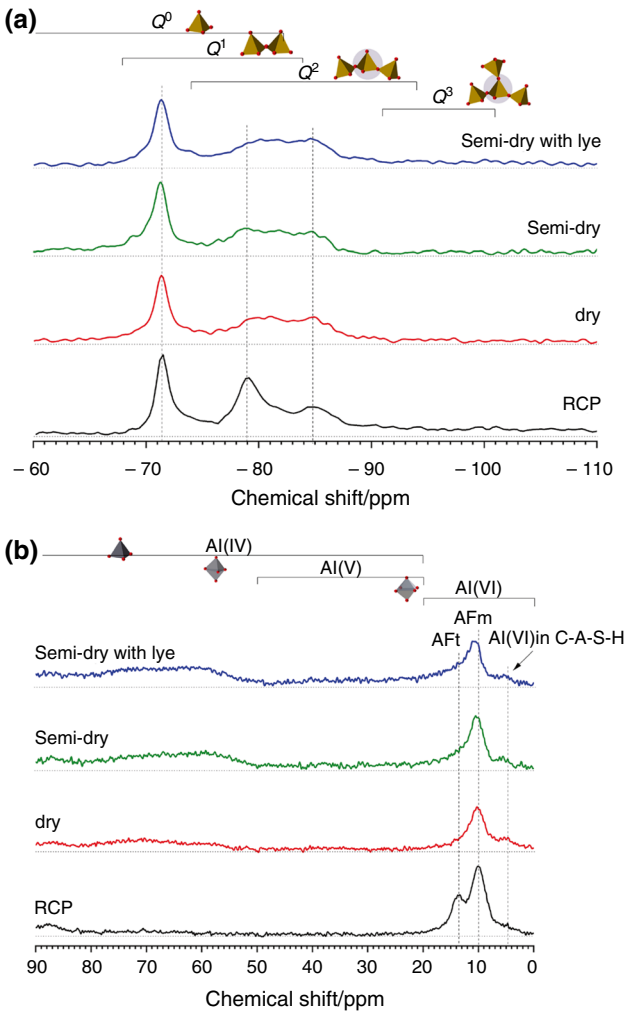

Fig. 3 **a** ^{29}Si NMR and **b** ^{27}Al NMR spectra of the carbonated (liquid–solid ratio of 0.1 for both the semi-dry methods and the carbonation time of 180 min) and uncarbonated RCP, all the spectra are normalized to reflect a constant total intensity

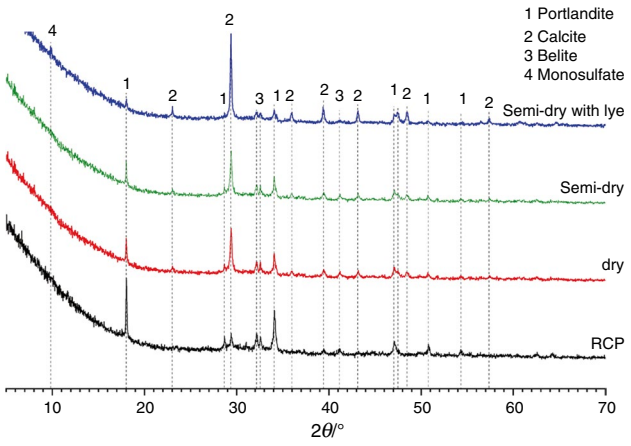

Fig. 4 XRD spectra of the carbonated (liquid–solid ratio of 0.1 for both the semi-dry methods and the carbonation time of 180 min) and uncarbonated RCP

the decalcification of the C-S-H gel and converted it into calcium carbonate and alumina–silica gel, as noted in reference [4]. The proportion of Q^0 and Q^1 species decreased, while the proportion of Q^2 species increased in all the cRCP after 180 min of carbonation. However, the expected Q^3 species was absent, pointing to incomplete decalcification of the C-S-H gel.

Al with coordination structure of fourfold, fivefold, or sixfold can be differentiated based on the chemical shift range observed in the ^{27}Al NMR spectrum (see Fig. 3b). However, there is some overlap in the range of 20–50 ppm, which is due to the presence of distorted fourfold-coordinated Al (Al(IV)) or fivefold-coordinated Al (Al(V)). The peaks observed at 13 ppm and 10 ppm in the spectrum can be attributed to ettringite and alumino-ferrite-mono (AFm) of the hydrocalumite subgroups, respectively [29]. The signal at around 5 ppm was less affected by the various carbonation methods. Previously assigned to third aluminate hydrate (TAH) with an unknown structure, it has recently been reported to be the signal of sixfold-coordinated Al (Al(VI)) in the calcium aluminum silicate hydrate (C-A-S-H) gel structure [30]. The findings suggest that C-A-S-H gel may exhibit slightly greater carbonation resistance than C-S-H gel, in line with a recent study on pure gels [31]. Other Al species in the spectra were identified as Al(IV), with a range of 20–90 ppm. It is evident that carbonation accelerated ettringite decomposition, as evidenced by a decrease in the peak at ~ 13 ppm. The existence of the amorphous alumina–silica gel was demonstrated by the dispersed peak in a range extending from 50 to 90 ppm. According to the variances in the ^{27}Al NMR spectra, the cRCP that underwent semi-dry techniques exhibited the most effective disintegration of ettringite and decalcified C-S-H gel.

The mineralogical composition of the RCP following various carbonation methods was investigated using XRD. The cRCP contained primarily calcite as well as a small quantity of portlandite and belite (see Fig. 4). The polymorph of calcite was not detected. The dry and semi-dry methods led to an increase in the calcite content in the cRCP. Among them, the semi-dry with lye method was identified as the most efficient way to convert portlandite into calcite, attributable to the effect of alkali [11]. Despite this, the total $CaCO_3$ content in the cRCP processed both by the semi-dry method and the semi-dry method with lye showed only marginal difference (Fig. 2b). The findings indicate that the alkaline environment in the RCP facilitated the formation of calcite, while having a minimal influence on the carbonation degree. This process had a lesser effect on portlandite [32]. The lack of an ettringite peak in the RCP diffractogram was due to mechanical grinding during sample preparation which

caused the conversion of ettringite to an XRD amorphous phase.

Reactivity of the cRCP in LC^3

Hydration kinetics of cementitious materials can be accurately monitored through heat flow. The heat flow can be simply divided into alite (tricalcium silicate or C_3S) and aluminate (tricalcium aluminate or C_3A) hydration, as shown in Fig. 5a. Initially, C_3A is passivated due to the rapid formation of calcium aluminate hydrate, once sulfate depletion occurs in the system (indicated by the onset of aluminate peak), desorbed sulfate ions accelerate C_3A dissolution and ettringite formation [33]. Furthermore, the initiation of the alite peak was determined through a two-stage process. First, the acceleration period within the heat flow between 1.0 and 2.0 mW g^{-1} was subjected to linear regression. Second, the hydration time at the intersection of the linear regression and the minimum heat flow, which exhibited a strong correlation with the initial setting of cementitious materials [34], was taken into account. It is justifiable to establish the linear regression within the heat flow between 0.5 and 1.0 mW g^{-1} in this research because the heat flow is adjusted to the mass of LC^3, which possesses a half alite component than Portland cement.

The semi-dry method treatment of RCP marginally amplified the heat of hydration of LC^3 after 24 h, when compared to limestone and other carbonation methods. Despite this, cRCP had a negligible impact on the heat of hydration of LC^3. The appearance of alite peak remained largely unaffected by the semi-dry method's treatment of RCP, whereas both dry and semi-dry with lye methods slightly delayed the onset and appearance of the peak. Similar results were observed in the appearance of the aluminate peak.

The impact of carbonation time on reactivity of cRCP was minimal, and there was very little discernible difference in

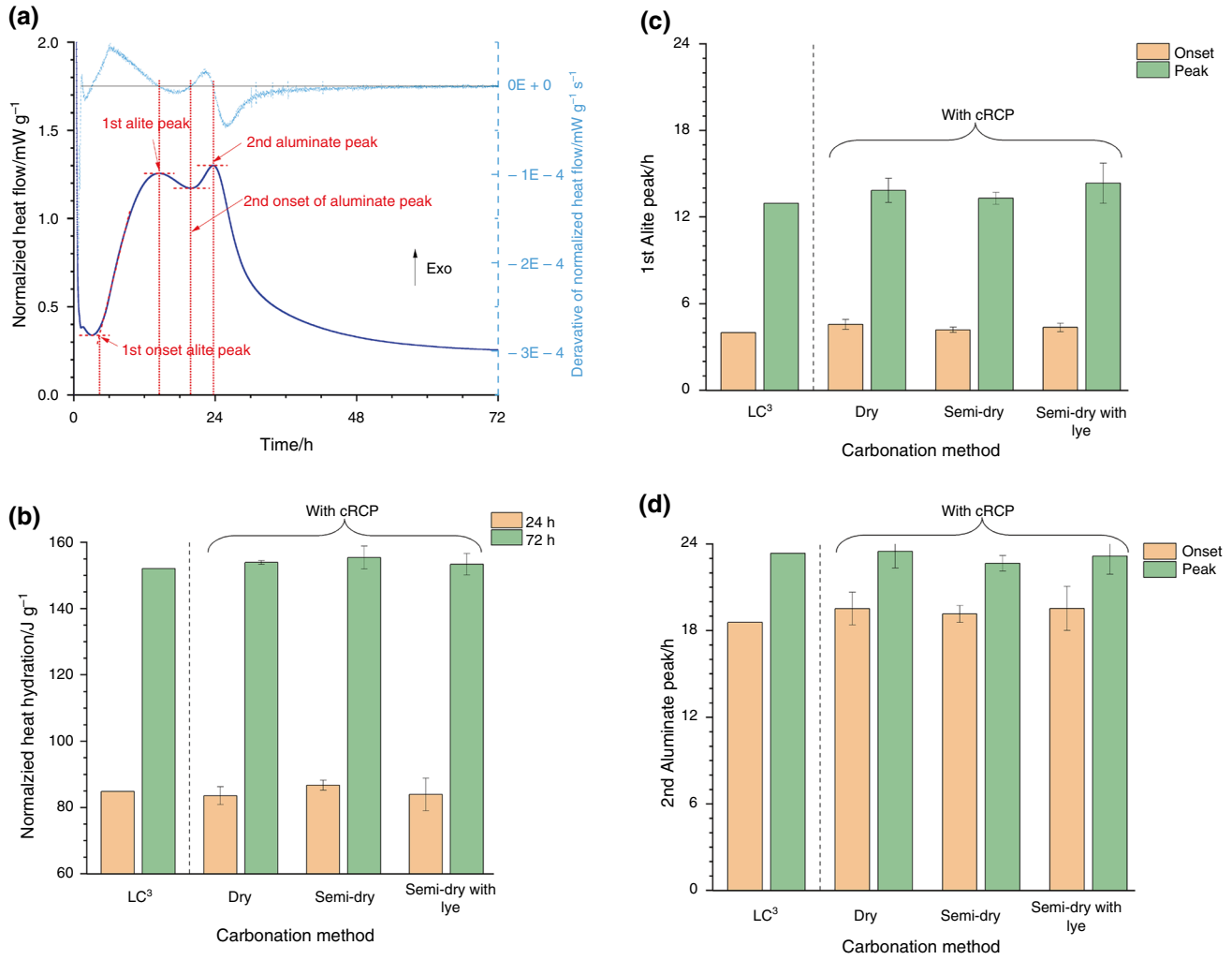

Fig. 5 **a** The timepoints in a typical heat flow curve of LC^3; **b** the heat of hydration and **c–d** the timepoints in the heat flow of LC^3 made from the cRCP plotted against different carbonation methods in the experiment design

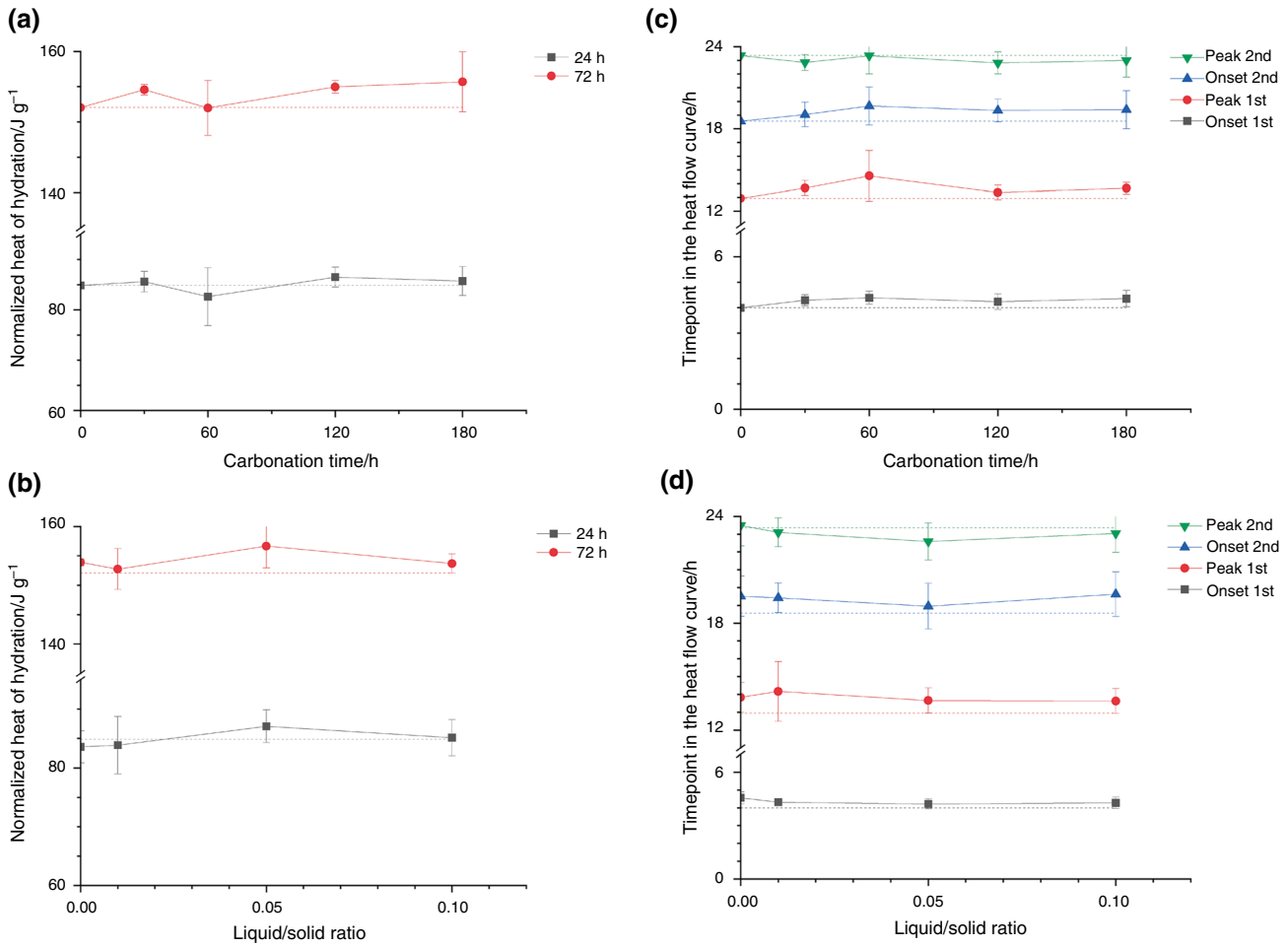

Fig. 6 **a**–**b** The heat of hydration and **c**–**d** the timepoints in the heat flow of the LC^3 made from the cRCP plotted against the carbonation time and the liquid–solid ratio in the experiment design

heat of hydration between LC^3 samples. The only noticeable variation was in the cRCP samples processed with 60-min carbonation, which released slightly less heat after 72 h, as shown in Fig. 6a. Additionally, the hydration kinetics of the samples were unaffected by variations in carbonation time for cRCP. The findings suggest that carbonation time does not significantly impact the reactivity of the cRCP in this experimental design. However, it is critical to note that a relatively large standard deviation is associated with the data from 60-min cRCP samples (Fig. 6a and Fig. 6c), indicating that the 60-min carbonation process might introduce significant compositional uncertainty to the cRCP.

Although liquid–solid ratio in the experiment design is fundamental in determining the $CaCO_3$ content of the cRCP, it barely influenced the reactivity. Only the cRCP, pre-wetted with 5% liquid (equivalent to a liquid–solid ratio of 0.05), resulted in a slight increase in the heat of hydration of the samples (Fig. 6b). Moreover, the hydration kinetics of the samples were not impacted by the cRCP. However, the samples containing the cRCP pre-wetted by 1% liquid display a relatively large standard deviation, as shown in Fig. 6d, suggesting that pre-wetting may introduce compositional uncertainty to the cRCP. To summarize, the aforementioned findings propose that the reactivity of LC^3 had only a slight impact from the cRCP. Nonetheless, pre-wetting, alkaline environment, and carbonation time affected the phase assemblage of the cRCP. A potential explanation is that a small amount of $CaCO_3$ was involved in the formation of calcium carboaluminate hydrates [35], while calcined clay supplied enough Al for the reaction and could either be incorporated into C-A-S-H gel or calcium carboaluminate hydrate [36]. Consequently, in this scenario, $CaCO_3$ and alumina–silica gel in the cRCP have a limited role in LC^3 reaction.

Conclusions

This study demonstrates that cRCP usage does not have any negative impact on LC^3 hydration, making it a viable substitute for limestone. LC^3 obtained from cRCP can be used

to produce a composite cement suitable for urban regions where cement consumption and CDW generation occur.

The increase in $CaCO_3$ content did not correspond proportionally with the decrease in $Ca(OH)_2$ content. This indicates that carbonation of $Ca(OH)_2$ was not the primary source of $CaCO_3$ incrementation in the cRCP. Therefore, the carbonation method needs further improvement to eliminate the densification effect of the carbonated products, such as utilizing periodic vibration during the carbonation process. The carbonation efficiency of the methods, ranked in descending order, is semi-dry with lye > semi-dry > dry. It was observed that pre-wetting of the RCP is crucial to ensure optimal carbonation efficiency as the $CaCO_3$ content escalates with the liquid/solid ratio. Both pre-wetting and an alkaline environment were advantageous for the decalcification of the hydration products and formation of $CaCO_3$ in the cRCP. To optimize processing efficiency, the use of alkali during pre-wetting is unnecessary. The reactivity of the cRCP in LC^3 did not demonstrate a significant correlation with either the $CaCO_3$ content or the phase assemblage, if sufficient reactive alumina or silica source was present. The utilization of cRCP proves beneficial for large-scale production of LC^3 due to its tolerance to the varying composition of cRCP.

Acknowledgements The authors gratefully acknowledge the financial supports of National Nature Science Foundation of China (52078301 and 52378251) and Department of Education of Guangdong Province (2021KTSCX283). Meanwhile, technique supports from Guangdong Provincial Key Laboratory of Durability for Marine Civil Engineering (SZU) (No. 2020B1212060074) are greatly acknowledged.

Author contributions Yu Jin and Yaocheng Wang helped in conceptualization; Yu Jin and Yaocheng Wang helped in methodology; Zihan Xiong and Weipeng Feng helped in formal analysis and investigation; Yu Jin and Zihan Xiong contributed to writing—original draft preparation; Weipeng Feng, Dapeng Zheng, Serina Ng, and Yaocheng Wang contributed to writing—review and editing; Yu Jin and Yaocheng Wang helped in funding acquisition; Serina Ng and Yaocheng Wang helped in resources; and Yu Jin and Yaocheng Wang worked in supervision.

Declarations

Conflict of interest The authors declared that there is no conflict of interest in content of this manuscript.

References

1. Dinga CD, Wen Z. China's green deal: can China's cement industry achieve carbon neutral emissions by 2060? Renew Sustain Energy Rev. 2022;155: 111931.
2. Scrivener KL, John VM, Gartner EM. Eco-efficient cements: Potential economically viable solutions for a low-CO2 cement-based materials industry. Cement Concrete Res. 2018;114:2–26.
3. Schoon J, de Buysser K, van Driessche I, de Belie N. Fines extracted from recycled concrete as alternative raw material for Portland cement clinker production. Cement Concrete Comp. 2015;58:70–80.
4. Zajac M, Skocek J, Skibsted J, Ben HM. CO_2 mineralization of demolished concrete wastes into a supplementary cementitious material – a new CCU approach for the cement industry. RILEM Tech Lett. 2021;6:53–60.
5. Aquino Rocha JH, Toledo Filho RD. The utilization of recycled concrete powder as supplementary cementitious material in cement-based materials: a systematic literature review. J Build Eng. 2023;76: 107319.
6. Zajac M, Skocek J, Durdzinski P, Bullerjahn F, Skibsted J, Ben HM. Effect of carbonated cement paste on composite cement hydration and performance. Cement Concrete Res. 2020;134: 106090.
7. Ben Ghacham A, Pasquier L-C, Cecchi E, Blais J-F, Mercier G. Valorization of waste concrete through CO_2 mineral carbonation: Optimizing parameters and improving reactivity using concrete separation. J Clean Prod. 2017;166:869–78.
8. Mehdizadeh H, Ling T-C, Cheng X, Pan S-Y, Hung MK. CO_2 Treatment of hydrated cement powder: characterization and application consideration. J Mater Civ Eng. 2021;33:4021041.
9. Zajac M, Skibsted J, Durdzinski P, Bullerjahn F, Skocek J, Ben HM. Kinetics of enforced carbonation of cement paste. Cement Concrete Res. 2020;131: 106013.
10 Zajac M, Skibsted J, Ben HM. Effect of alkalis on enforced carbonation of cement paste: mechanism of reaction. J Am Ceram Soc. 2020;131:106013.
11. Zajac M, Skibsted J, Durdzinski P, Ben HM. Effect of alkalis on products of enforced carbonation of cement paste. Constr Build Mater. 2021;291: 123203.
12 Zajac M, Skibsted J, Bullerjahn F, Skocek J. Semi-dry carbonation of recycled concrete paste. J CO2 Util. 2022;63:102111.
13. Zajac M, Skocek J, Ben Haha M, Dienemann W. Performance and hydration of ternary cements based on Portland clinker, carbonated recycled concrete paste (cRCP) and calcined clay. J Sustainable Cem-Based Mater. 2024;13:338–50.
14. Rocha JHA, Toledo Filho RD. Microstructure, hydration process, and compressive strength assessment of ternary mixtures containing Portland cement, recycled concrete powder, and metakaolin. J Clean Prod. 2024;434: 140085.
15. Scrivener K, Martirena F, Bishnoi S, Maity S. Calcined clay limestone cements (LC^3). Cement Concrete Res. 2018;114:49–56.
16. Sánchez Berriel S, Favier A, Rosa Domínguez E, Sánchez Machado IR, Heierli U, Scrivener K, et al. Assessing the environmental and economic potential of limestone calcined clay cement in Cuba. J Clean Prod. 2016;124:361–9.
17. Lu W, Webster C, Peng Y, Chen X, Zhang X. Estimating and calibrating the amount of building-related construction and demolition waste in urban China. Int J Constr Manag. 2017;17:13–24.
18. Sharma M, Bishnoi S, Martirena F, Scrivener K. Limestone calcined clay cement and concrete: a state-of-the-art review. Cement Concrete Res. 2021;149: 106564.
19. Wadsö L, Winnefeld F, Riding KA, Sandberg PJ. Chapter 2 Calorimetry. In: Scrivener KL, Snellings R, Lothenbach B, editors. A practical guide to microstructural analysis of cementitious materials. Boca Raton: CRC Press; 2016. p. 37–74.
20. Baran T, Pichniarczyk P. Correlation factor between heat of hydration and compressive strength of common cement. Constr Build Mater. 2017;150:321–32.
21 Alujas Diaz A, Almenares Reyes RS, Hanein T, Irassar EF, Juenger M, Kanavaris F, et al. Properties and occurrence of clay resources for use as supplementary cementitious materials: a paper of RILEM TC 282-CCL. Mater Struct. 2022. https://doi.org/10.1617/s11527-022-01972-2.

22. Zheng D, Liang X, Cui H, Tang W, Liu W, Zhou D. Study of performances and microstructures of mortar with calcined low-grade clay. Constr Build Mater. 2022;327: 126963.
23. Lothenbach B, Durdziński PT, de Weerdt K. Chapter 5 Thermogravimetric analysis. In: Scrivener KL, Snellings R, Lothenbach B, editors. A practical guide to microstructural analysis of cementitious materials. Boca Raton: CRC Press; 2016. p. 178–213.
24. Lu B, Shi C, Zhang J, Wang J. Effects of carbonated hardened cement paste powder on hydration and microstructure of Portland cement. Constr Build Mater. 2018;186:699–708.
25. Steinour HH. Some effects of carbon dioxide on mortars and concrete-discussion. J Am Concrete. 1959;I(30):905–7.
26. Kangni-Foli E, Poyet S, Le Bescop P, Charpentier T, Bernachy-Barbé F, Dauzères A, et al. Carbonation of model cement pastes: The mineralogical origin of microstructural changes and shrinkage. Cement Concrete Res. 2021;144: 106446.
27. Morandeau A, Thiéry M, Dangla P. Investigation of the carbonation mechanism of CH and C-S-H in terms of kinetics, microstructure changes and moisture properties. Cement Concrete Res. 2014;56:153–70.
28. Walkley B, Provis JL. Solid-state nuclear magnetic resonance spectroscopy of cements. Mater Today Adv. 2019;1: 100007.
29. Skibsted J. Chapter 6 High-resolution solid-state nuclear magnetic resonance spectroscopy of portland cement-based systems. In: Scrivener KL, Snellings R, Lothenbach B, editors. A practical guide to microstructural analysis of cementitious materials. Boca Raton: CRC Press; 2016. p. 214–86.
30. Kunhi Mohamed A, Moutzouri P, Berruyer P, Walder BJ, Siramanont J, Harris M, et al. The atomic-level structure of cementitious calcium aluminate silicate hydrate. J Am Chem Soc. 2020;142:11060–71.
31. Liu X, Feng P, Cai Y, Yu X, Liu Q. Carbonation behaviors of calcium silicate hydrate (C-S-H): Effects of aluminum. Constr Build Mater. 2022;325: 126825.
32. Winnefeld F, Schöler A, Lothenbach B. Chapter 1 Sample preparation. In: Scrivener KL, Snellings R, Lothenbach B, editors. A practical guide to microstructural analysis of cementitious materials. Boca Raton: CRC Press; 2016. p. 1–36.
33. Zunino F, Scrivener KL. The influence of the filler effect on the sulfate requirement of blended cements. Cement Concrete Res. 2019;126: 105918.
34. von Daake H, Stephan D. Setting of cement with controlled superplasticizer addition monitored by ultrasonic measurements and calorimetry. Cement Concrete Comp. 2016;66:24–37.
35. Vizcaíno Andrés LM, Antoni MG, Alujas Diaz A, Martirena Hernández JF, Scrivener KL. Effect of fineness in clinker-calcined clays-limestone cements. Adv Cem Res. 2015;27:546–56.
36. Avet F, Scrivener K. Investigation of the calcined kaolinite content on the hydration of limestone calcined clay cement (LC^3). Cement Concrete Res. 2018;107:124–35.